

Integrated Bandpass Filter at 77 GHz in SiGe Technology

Bernhard Dehlink, *Student Member, IEEE*, Mario Engl, Klaus Aufinger, and Herbert Knapp, *Member, IEEE*

Abstract—The implementation and characterization of an integrated passive bandpass filter at 77 GHz is presented. A lumped elements filter occupying very small die area ($110 \times 60 \mu\text{m}^2$, without pads) is demonstrated. It is realized with spiral inductors and metal-insulator-metal capacitors. The filter is fabricated in an advanced SiGe:C technology. It has a center frequency of 77.3 GHz and a bandwidth of 12 GHz. The insertion loss is 6.4 dB. This is the first time that integrated inductors are used for filters at millimeter wave frequencies around 80 GHz.

Index Terms—Automotive radar, bandpass filters (BPFs), broadband communication, lumped element microwave circuits, millimeter wave radar, silicon germanium (SiGe).

I. INTRODUCTION

AUTOMOTIVE radar at a target frequency of 77 GHz and broadband communication applications around 80 GHz are the driving force behind SiGe technology and circuit development [1]–[3]. The frequency band from 76 GHz to 77 GHz is assigned to long range radar (LRR) that covers distances up to 200 m. The bands from 71 to 76 GHz and 81 to 86 GHz can be used for communication purposes. A point of great concern in heterodyne receivers is the suppression of spectral components at the image frequency [4]. Using bandpass filters (BPFs) in such systems reduces the noise at the image frequency, which lowers the receiver noise figure.

The feasibility of lumped inductors and transformers at millimeter wave frequencies has been successfully demonstrated in [5]. A 65-GHz receiver where inductors are used in the LNA, the mixer, and the VCO, is shown in [6].

Integrated filter realizations are rare at millimeter wave frequencies close to 100 GHz. Interesting work is reported in [7] and [8]. In [7], a third-order Chebyshev BPF at 77 GHz was implemented in a $0.25 \mu\text{m}$ BiCMOS technology using transmission lines. The center frequency is at 75.8 GHz. The insertion loss varies between 4.8 dB and 6.8 dB in the passband. The filter is designed for a 3-dB bandwidth of 21 GHz, or 28%. In [8], an inductive coupled coplanar filter on a quartz wafer with gold metallization is presented. At a center frequency of 97 GHz, this filter has an insertion loss of 2.7 dB and a 3-dB bandwidth of 10%. However, these filters are based on distributed elements, occupying large chip areas. The filter in [8]

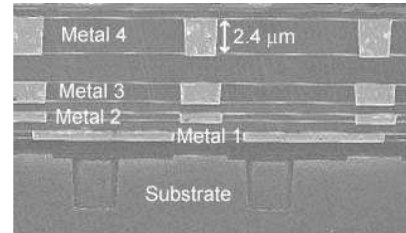


Fig. 1. Cross-sectional view of the metal stack.

needs $1644 \times 530 \mu\text{m}^2$, the one in [7] roughly $195 \times 70 \mu\text{m}^2$. So the main design goals for the circuit presented in this letter were minimum area consumption without compromising the performance.

A single resonator has a passband insertion loss [9]

$$\text{IL} = 20 \log_{10} \frac{Q_U}{Q_U - Q_L} \quad [\text{dB}]. \quad (1)$$

Here, $Q_L = (f_c/BW)$ is the loaded quality factor, where f_c and BW are the center frequency and the 3-dB bandwidth, respectively. The unloaded quality factor of an inductor (capacitor) is defined as $Q_U = (X/R)$, where X stands for the reactance and R is the resistance. It is apparent that a filter with a very narrow bandwidth (large Q_L) is usually not implementable since an unrealistic high quality factor Q_U would be needed for an acceptable insertion loss.

The filter presented in this letter was implemented in an advanced SiGe technology [1]. This technology provides four copper metallization layers. A photograph of the metal stack is shown in Fig. 1. The topmost layer (Metal 4) over silicon substrate (resistivity $18.5 \Omega\text{cm}$) was used for the design of the inductors. This reduces the electrical coupling into the substrate. The distance of Metal 4 from the substrate is $7.1 \mu\text{m}$.

II. LUMPED ELEMENTS FILTER

Equation (1) defines the insertion loss of a resonator. To keep the loss low, a bandwidth of 10 GHz at a center frequency of 76.5 GHz was chosen. This leaves Q_L at a value that can be implemented, 7.65. The design is based on a Butterworth characteristic. The schematic is depicted in Fig. 2. The implemented design has two resonant structures (L_1C_1 and L_2C_2). The values for the capacitances are 56 fF for $C_{1,2}$, and the inductances $L_{1,2}$ both have a value of 47 pH. The other capacitors have values of 27 fF ($C_{3,4}$) and 12.5 fF (C_5). A precise model for the stray capacitance must be included for capacitors with values below 30 fF. Series connections of larger capacitors were used to avoid this problem. In the layout, capacitor C_5 consists of a series connection of four metal-insulator-metal

Manuscript received November 7, 2006; revised December 21, 2006.

B. Dehlink is with Infineon Technologies AG, Neubiberg D-85579, Germany and also with the Radio Frequency Engineering group at the Vienna University of Technology, 1040 Vienna, Austria (e-mail: bernhard.dehlink@infineon.com).

M. Engl, K. Aufinger, and H. Knapp are with Infineon Technologies AG, Neubiberg D-85579, Germany.

Color versions of one or more of the figures in this paper are available online at <http://ieeexplore.ieee.org>.

Digital Object Identifier 10.1109/LMWC.2007.895701

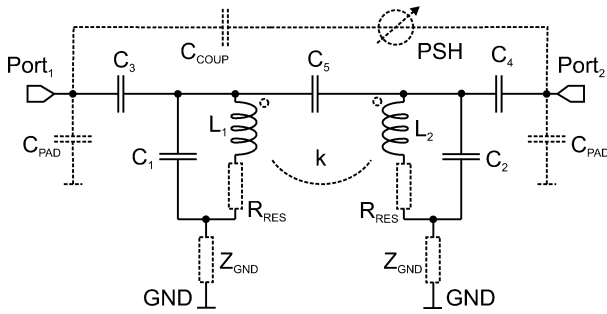


Fig. 2. Schematic of the lumped elements filter. The dashed symbols represent the parasitic elements.

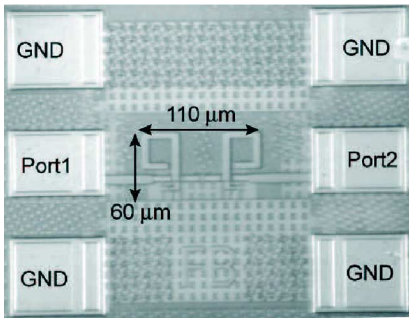


Fig. 3. Photograph of the lumped elements filter. Chip size including pads is $290 \times 370 \mu\text{m}^2$.

(MIM) capacitors with a value of 50 fF each. Capacitors $C_{3,4}$ are implemented using two 54-fF capacitors in series. The most important parasitics are depicted in Fig. 2 using dashed lines. They represent a physical model. The values for the parasitics were obtained by extraction from the measured data. All capacitive coupling effects are combined in the capacitor C_{COUP} and the phase shifter PSH. The coupling coefficient of the coils is denoted with k . The resonator's resistance is $R_{\text{RES}} = 1.6 \Omega$. The connection of the resonator to the ground pads is modeled by Z_{GND} . The pad capacitances C_{PAD} , which amount to 17.7 fF each, contribute mainly to the input and output matching. The pad size is $50 \mu\text{m}^2$.

A photograph of the implemented filter is depicted in Fig. 3. The chip as shown in this figure measures $290 \times 370 \mu\text{m}^2$. The filter structure without pads needs only $110 \times 60 \mu\text{m}^2$.

Integrated inductors are used for filters in this frequency range for the first time. Their dimensions were calculated using FastHenry [10]. This tool yields good results even at millimeter wave frequencies. The inductors consist of one turn. They have an inner diameter of $22 \mu\text{m}$ and a conductor width of $5 \mu\text{m}$. They are implemented using Metal 4 over substrate. This yields an inductance of 47 pH at 77 GHz. The simulated quality factor of the coils at the same frequency is 19. The simulated frequency behaviors of the inductance and the quality factor are shown in Fig. 4. The parasitic capacitances of the coils are the metal-substrate capacitances solely, since the coils have one turn only. These capacitances have a value of 6.5 fF each. The simulated self-resonant frequency of the coils is well above the maximum simulated frequency.

The measurement results of the BPF are depicted in Fig. 5. Only S_{11} and S_{21} are shown since the filter is symmetrical.

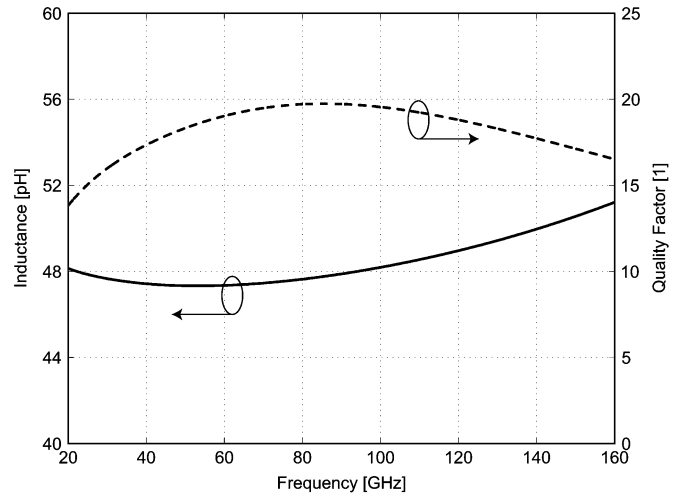


Fig. 4. Simulated (HFSS) inductance and quality factor of one coil versus frequency. At the center frequency (77 GHz), the inductance is 47 pH and the quality factor is 19.

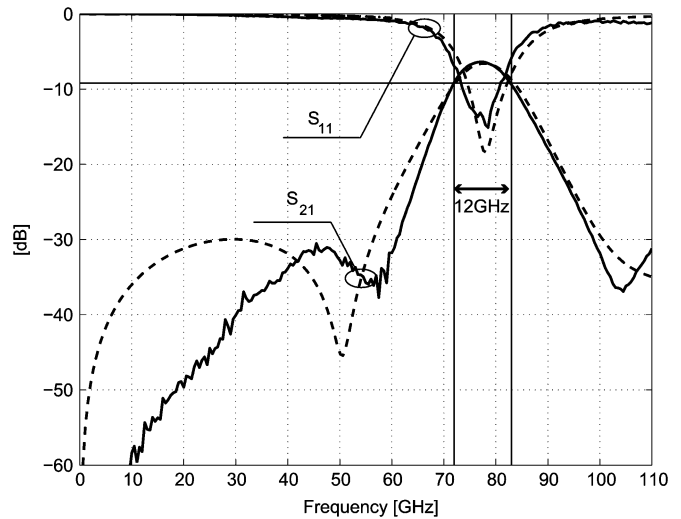


Fig. 5. Measured (solid lines) and simulated S -parameters of the lumped elements filter. The dashed line represents the simulation including all parasitics shown in Fig. 2.

The center frequency of the filter, $f_c = \sqrt{f_u \cdot f_l}$, is 77.3 GHz. Here, f_u and f_l are the upper and lower 3 dB cut-off frequency, respectively. The 3-dB bandwidth, $\text{BW} = f_u - f_l$, is 12 GHz, or 15.5%. This leads to $Q_L = 6.4$. The minimum insertion loss is 6.4 dB. The simulation results including parasitics are shown in the same plot (dash-dotted line). Without the parasitics, S_{21} does not exhibit the notches at 60 GHz and at 105 GHz, thus the transitions from passband to stopband are not as steep as measured. The filter's behavior at frequencies higher than the center frequency is mostly determined by the magnetic coupling of the two coils. Especially the notch at 105 GHz is modeled in this way. The value of the coupling coefficient k is 0.26, which is equal to a mutual inductance of 11.7 pH. The impedance Z_{GND} contributes to the depth and the position of the notch at 105 GHz. In addition, the behavior of S_{21} at frequencies higher than 110 GHz depends heavily on it. This parasitic impedance includes the inductance of the ground connections (15 pH). The inductance results from the narrow paths of the resonators

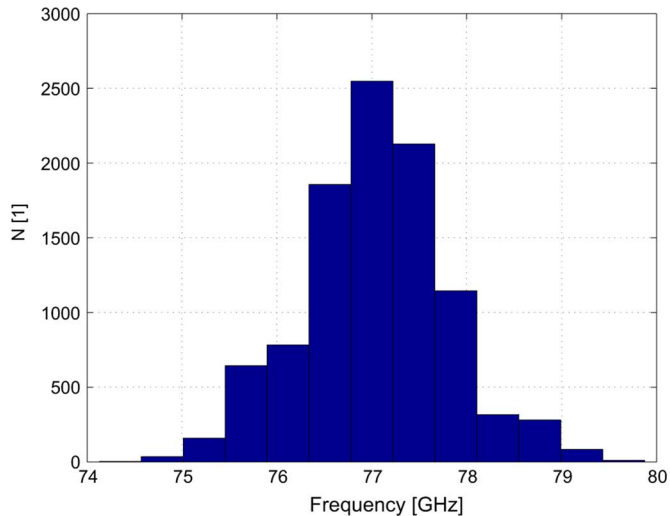


Fig. 6. Variation of center frequency of the BPF due to process variations (Monte Carlo simulation, 10 000 runs).

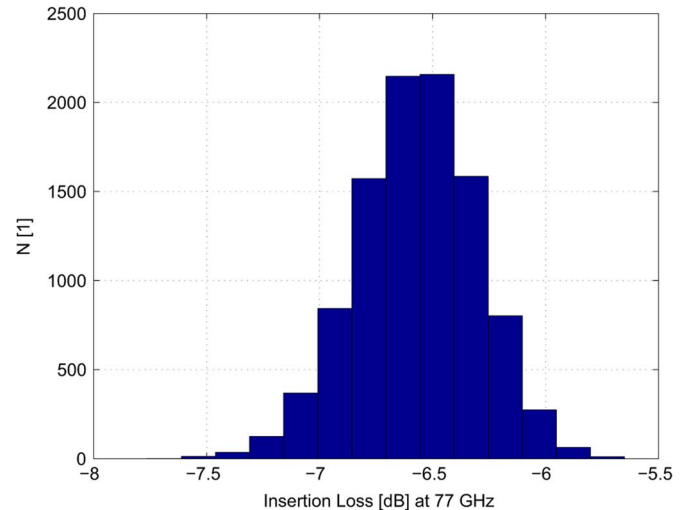


Fig. 7. Variation of insertion loss at center frequency due to process variations (Monte Carlo simulation, 10 000 runs).

$LC_{1,2}$ to ground. This measure is needed to keep any metal layer away from the inductors to leave the magnetic field undistorted. The capacitive coupling of the coil into the substrate is much smaller than $C_{1,2}$ (6.5 fF). This capacitance is included in $C_{1,2}$ in Fig. 2. At low frequencies, the insertion of $C_{COUP} = 2$ fF and PSH (44°) results in the notch at 50 GHz. With the main parasitics included, a close match between the simulated and the measured data is obtained for frequencies at and above the passband. At lower frequencies, the shortcomings of this model become apparent.

Process variations result in variations of the filter characteristics. The capacitance of MIM capacitors is assumed to vary up to 10% (3σ). This is a typical value for the used process. The fabrication tolerance of the metallization layers impacts mainly the series resistance of the coils. The change of the inductance is negligible. The robustness of the filter versus these process variations is investigated by a Monte Carlo simulation. The resulting center frequency variations are shown in Fig. 6. Fig. 7 shows the variations of the insertion loss at the nominal center frequency, which is 77 GHz. The depicted results show that 98.6% of the simulated center frequency values lie within 77 ± 2 GHz. The insertion loss is smaller than 7 dB (nominal 6.4 dB) in 94.6%, and the bandwidth stays within 12.5 ± 1 GHz for 99.8% of all realizations. This indicates that process variations have a minor impact on the filter performance.

III. CONCLUSION

We successfully demonstrate the implementation of a millimeter wave BPF. The lumped elements filter uses two LC parallel resonant circuits. It has a center frequency of 77.3 GHz, a 3-dB bandwidth of 12 GHz, and a minimum insertion loss of 6.4 dB. In the design and the layout of the filter, attention

must be paid to parasitic coupling that affects the frequency response. Simulations show that this BPF is very robust against process variations. The filter occupies a small chip area of $110 \times 60 \mu\text{m}^2$. Thus, lumped elements are good alternatives to microstrip realizations at millimeter wave frequencies.

REFERENCES

- [1] J. Böck, H. Schäfer, H. Knapp, K. Aufinger, M. Wurzer, S. Boguth, T. Böttner, R. Stengl, W. Perndl, and T. F. Meister, "3.3 ps SiGe bipolar technology," in *IEDM Tech. Dig.*, 2004, pp. 255–258.
- [2] H. Li, H.-M. Rein, T. Suttorp, and J. Böck, "Fully integrated SiGe VCOs with powerful output buffer for 77-GHz automotive radar systems and applications around 100 GHz," *IEEE J. Solid State Circuits*, vol. 39, no. 4, pp. 1650–1658, Oct. 2004.
- [3] B. Dehlink, H.-D. Wohlmut, K. Aufinger, T. F. Meister, J. Böck, and A. L. Scholtz, "A low-noise amplifier at 77 GHz in SiGe:C bipolar technology," in *IEEE Compound Semicond. Integr. Circuit (CSIC) Symp. Tech. Dig.*, Palm Springs, FL, Oct.–Nov. 2005, pp. 287–290.
- [4] S. K. Reynolds, B. A. Floyd, U. R. Pfeiffer, T. Beukema, J. Grzyb, C. Haymes, B. Gaucher, and M. Soyuer, "A silicon 60-GHz receiver and transmitter chipset for broadband communications," *IEEE J. Solid State Circuits*, vol. 41, no. 12, pp. 2820–2831, Dec. 2006.
- [5] T. O. Dickson, M.-A. LaCroix, S. Boret, D. Gloria, R. Beerkens, and S. P. Voinescu, "30–100-GHz inductors and transformers for millimeter-wave (Bi)CMOS integrated circuits," *IEEE Trans. Microw. Theory Tech.*, vol. 53, no. 1, pp. 123–133, Jan. 2005.
- [6] M. Gordon, T. Yao, and S. P. Voinescu, "65-GHz receiver in SiGe BiCMOS using monolithic inductors and transformers," in *IEEE Topical Meeting Silicon Monolith. Integr. Circuits RF Syst. (SiRF) Tech. Dig.*, San Diego, CA, Jan. 2006, pp. 265–268.
- [7] E. van der Heijden, M. Notten, G. Dolmans, H. Veenstra, and R. Pijper, "On-chip third-order band-pass filters for 24 and 77 GHz car radar," in *Int. Microw. Symp. (IMS) Tech. Dig.*, San Francisco, CA, Jun. 2006, pp. 697–670.
- [8] F. Aryanfar and K. Sarabandi, "Characterization of semilumped CPW elements for millimeter-wave filter design," *IEEE Trans. Microw. Theory Tech.*, vol. 53, no. 4, pp. 1288–1293, Apr. 2005.
- [9] R. W. Rhea, "High-Q resonators on FR4," *Appl. Microw. Wireless*, pp. 64–65, Oct. 1999.
- [10] "FastHenry USER's GUIDE, Version 3.0," Mass. Inst. Technol., Cambridge, MA, 1996.